Direct Determination of Changes of Interdomain Orientation on Ligation: Use of the Orientational Dependence of ^{15}N NMR Relaxation in Abl SH(32)†

David Fushman, Rong Xu, and David Cowburn*

The Rockefeller University, 1230 York Avenue, New York, New York 10021

Received April 19, 1999; Revised Manuscript Received June 7, 1999

ABSTRACT: The relative orientation and motions of domains within many proteins are key to the control of multivalent recognition, or the assembly of protein-based cellular machines. Current methods of structure determination have limited applicability to macromolecular assemblies, characterized by weak interactions between the constituents. Crystal structures of such complexes might be biased by packing forces comparable to the interdomain interactions, while the precision and accuracy of the conventional NMR structural approaches are necessarily limited by the restricted number of NOE contacts and by interdomain flexibility rendering the available NOE information uninterpretable. NMR relaxation studies are capable of providing "long-range" structural information on macromolecules in their native milieu. Here we determine directly the change in domain orientation between unligated and dual ligated subdomains of the SH(32) segment of Abelson kinase in solution, using the orientational dependence of nuclear spin relaxation. These results demonstrate that the change in domain orientation between unligated and ligated forms can be measured directly in solution.

Current methods of high-resolution structure determination are generally applicable to macromolecular assemblies formed by tight contacts between the individual, well-structured components. These methods have more limited applicability in those cases where there are weaker interactions between the constituents; examples include the relatively transient associations formed in complexes involved in signal transduction, or in transcriptional control. Crystal structures of such complexes might be biased by packing forces comparable to the interdomain interactions, while the precision and accuracy of the conventional NMR structural approaches are necessarily limited by the restricted number of NOE[1] contacts and by interdomain flexibility rendering the available NOE information uninterpretable. Novel NMR approaches proposed recently (*1*−*5*) are potentially capable of improving both the accuracy and precision of structure determination in solution and might prove to be the method of choice in those cases when the number of available short-range NOE contacts is limited. These methods are based on "long-range" structural information in the form of internuclear vector constraints with respect to an overall, molecular reference frame. These constraints may arise from correlation with the anisotropic hydrodynamic properties of the molecule (*2*−*4*) or from weak alignment of molecules in solution caused either by their interaction with the magnetic field (*1*) or by the liquid crystalline characteristics of the medium (*5*). The NMR relaxation approach (*2*−*4*), which takes advantage of the anisotropic character of the overall rotation, is most generally applicable to a wide range of macromolecules in their native milieu. The magnetic alignment method (*1*, *6*) requires macromolecules to possess a sufficiently high anisotropy of the magnetic susceptibility and is not, therefore, widely applicable. The approaches based on weak alignment of macromolecules in liquid crystalline medium may be restricted by possible interactions between the molecule under investigation and the medium. For a list of intractable target proteins by this method using lipid bicelles, see footnote 8 in ref *7*, although more recent alignment methods may alleviate this issue (*7*−*10*). We demonstrate here that the NMR relaxation approach can be extended to determine directly the change of domain orientation between unligated and dual ligated subdomains of the SH(32) fragment of Abelson kinase.

Src homology (SH) domains are modular protein domains widely distributed among proteins involved in intracellular signal transduction. SH2 domains recognize short peptidic segments containing phosphotyrosine, and SH3 domains bind to proline-rich segments forming a short helical turn in the complexes (*11*). While the individual structural properties and ligand specificities of these domains are fairly well understood, the structural organization and interactions between them in the multidomain complexes are complex and difficult to elucidate. These interactions are likely to be of significance, in particular, in view of the frequency of protein constructs containing adjacent SH2 and SH3 domains. Examples of structural studies of the multiple SH3/SH2 domain constructs are Lck SH(32), Grb2 SH(323), Abl SH(32), Hck SH(321), and Src and Src SH(32) (reviewed in refs *11* and *12*). Structural approaches to these complexes are complicated by the limited contacts and energies of the interdomain interactions. While the crystal structures of the

† This work was supported by National Institutes of Health Grant GM-47021(D.C.) and Fellowship AI-09537 (R.X.).

* To whom correspondence should be addressed. Telephone: (212) 327-8270. Fax: (212) 327-7566. E-mail: cowburn@rockefeller.edu.

[1] Abbreviations: Abl, Abelson protein tyrosine kinase; SH(32), dual domain of SH3 and SH2; SH3, src homology 3 domain; SH2, src homology 2 domain; R_1, longitudinal relaxation rate; R_2, transverse relaxation rate; NOE, nuclear Overhauser effect.

10.1021/bi990897g CCC: $18.00
Published on Web 07/23/1999

src-family SH(321) kinase systems have shed significant insight into unexpected kinases/SH3 interactions and demonstrated the allosteric nature of kinase inhibition by intramolecular phosphorylation, these structures of the downregulated, inactive forms of the enzymes do not provide a detailed understanding of the mechanism of regulation or the roles of domains in substrate recognition (*12*, *13*). This issue of interdomain flexibility in solution is a general one for large multidomain proteins (*14*).

In this paper, we characterize the relative orientation of the SH2 and SH3 domains in the SH(32) dual domain construct from human Abelson protein tyrosine kinase (Abl) in solution, free, and in ligated form. The human enzyme is protooncogenic for chronic myologenous leukemia, caused by chromosomal translocation, leading to disordering of the normal downregulated kinase (*15*). A dual domain system is the simplest model for multidomain proteins and thus is an archetypal system for the relative reorientation of the individual domains in multidomain proteins. In Abl SH(32), the two domains are separated by a six-residue native-sequence linker. The crystal structure of unligated Abl SH(32) (*16*) shows significant intramolecular contacts between the two domains, in particular, at the BC loop of SH2, which is involved in phosphotyrosine binding. On the other hand, solution studies (*17*−*19*) indicate that there are few interdomain contacts in solution and that the binding sites are completely independent. This apparent controversy illustrates the difficulties of understanding these kinds of systems fully. The NOESY NMR spectra of Abl SH(32) provide a negligible amount of information on possible contacts between the domains, certainly not sufficient to determine their relative orientation in the Abl SH(32). The NMR relaxation approach turns out to be the only available source of information on the dual domain structure in the free state and complexed with a consolidated ligand. As a model of possible ligation for multidomain proteins, we have previously demonstrated that "consolidated ligands", incorporating individual ligands for SH3 and SH2 domains tethered by an oligoglycyl linker, bind with enhanced affinity to SH(32) (*19*, *20*). These consolidated ligands provide an opportunity to turn on and off the relative motion of the domains and to study their interaction and its effect on the multiple domain motion.

In this paper, we present a modified, improved calculation of the rotational diffusion axes from ratios of relaxation times and derive the orientations of the domains in SH(32) in both unligated and ligated states. A significant change of orientation is thereby directly observed in solution.

MATERIALS AND METHODS

Experimental Procedures. Protein and ligand preparation and NMR structure determination of the individual domains have been reported previously (*17*, *21*). NMR signal assignment for both free and complexed states of Abl SH(32) is reported in ref *22*. The backbone ^{15}N relaxation parameters, comprising the rates of ^{15}N transverse (R_2) and longitudinal (R_1) relaxation and the ^{15}N{^{1}H} steady-state NOE, were measured on a Bruker DMX600 using previously described experimental protocols (*23*). Protein concentration in phosphate-buffered saline was ~1.5 mM for the SH3, 3 mM for the SH2, and 500 μM for the free and 600 μM for the ligated SH(32); the pH was adjusted to 7.2, and the sample temperature was 31 °C. The consolidated ligand comprised individual ligands for the SH2 and SH3 domains, NH_2-PVpYENVG$_6$>(PPAYAPPPVK-$CONH_2$), where ">" denotes that the C-terminal glycyl residue is linked to the N$^\epsilon$ of lysyl in the second peptide segment (*19*).

Data Analysis. The relaxation rates were modified to subtract contributions from the high-frequency components (P_{HF}) of local motion (*24*, *25*) as follows: $R_1' = R_1 - 6.25P_{HF}$; $R_2' = R_2 - 5.39P_{HF}$, where $P_{HF} = (|\gamma_N|/\gamma_H)(1 - \text{NOE})R_1/5$ and γ_N and γ_H are gyromagnetic ratios for ^{15}N and ^{1}H. These equations were obtained from the standard expressions (*26*) under the assumption that the spectral density function scales as $J(\omega) \propto \omega^{-2}$ at $\omega \approx \omega_H$ (*27*).

Determination of the Overall Rotational Diffusion Tensor. Anisotropic rigid-body rotations of the molecule in general can be characterized by a rotational diffusion tensor D having three principal values, D_{xx}, D_{yy}, and D_{zz}. Assuming an axially symmetric overall rotational diffusion tensor (characterized by the principal values $D_\parallel \equiv D_{zz}$ and $D_\perp \equiv D_{xx} = D_{yy}$) considered here, the dependence of the R_2'/R_1' ratio on the angle θ between the NH vector and the unique axis of the tensor can be represented, using the expressions of ref *28*, as follows:

$$\left(\frac{2R_2'}{R_1'} - 1\right)^{-1} = \frac{3/4}{1+(\omega_N\tau_1)^2}\left\{1 + \frac{(\omega_N\tau_1)^2}{(\omega_N\tau_1)^2 + \left(1+\frac{1}{6}\epsilon\right)^2} \times \frac{\epsilon \sin^2\theta}{3 + 2\epsilon + \left[1+\frac{1}{3}\epsilon(2-3\sin^2\theta)\right]^2}\left[4 + 3\epsilon + \frac{2}{9}\epsilon^2 - \epsilon\sin^2\theta\left(1 + \frac{4+\frac{11}{3}\epsilon+\frac{19}{18}\epsilon^2+\frac{5}{54}\epsilon^3}{(\omega_N\tau_1)^2+\left(1+\frac{2}{3}\epsilon\right)^2}\right)\right]\right\} \quad (1)$$

where $\epsilon \equiv D_\parallel/D_\perp - 1$, $\tau_1^{-1} \equiv 6D_\perp$, and ω_N is the ^{15}N resonance frequency. An overall rotational correlation time τ_c can be defined as $\tau_c^{-1} \equiv 6\ \text{tr}(D/3) = 2(D_\parallel + 2D_\perp)$. Equation 1 is exact in the absence of local motion and chemical exchange. It provides a good approximation for the protein core residues, characterized by restricted mobility in the protein backbone, and is more general than those used previously (*29*, *30*), which are valid only for small anisotropies ($\epsilon < 1$) and for $\omega_N\tau_1 \gg 1$. This then extends the approach to accommodate small, fast-tumbling molecules (e.g., $\omega_N\tau_1 \sim 1.7$ for the free Abl SH3 domain) and molecules with significant rotational anisotropy. We have shown separately (*31*) that possible changes in R_2'/R_1' due to modulation of the residue-specific ^{15}N chemical shift anisotropy tensor (*24*, *25*) are small for the axial ratios determined here and may be neglected.

Orientation of the principal axes of the diffusion tensor is given by the set of three Euler angles: Φ, Θ, and Ψ. Ψ is treated as zero for the assumed axial symmetry. The remaining two angles were determined, together with $D_\parallel$ and $D_\perp$, by minimizing the difference between the measured (exp)

and calculated (calc) values of $f_i = 1/(2R_{2i}'/R_{1i}' - 1)$, using the following target function: $E = \sum_{i=1}^{N_r}[(f_i^{exp} - f_i^{calc})/\sigma_i]^2$, where N_r is the total number of residues included in the analysis and σ_i denotes the experimental error in f_i for residue i. f_i^{calc} was obtained using eq 1, with the θ angle determined as $\theta = \cos^{-1}(\lambda_{ix} \cos \Phi \sin \Theta + \lambda_{iy} \sin \Phi \sin \Theta + \lambda_{iz} \cos \Theta)$, where $\{\lambda_{ix}, \lambda_{iy}, \lambda_{iz}\}$ are coordinates of a unit vector in the direction of the NH_i bond. To minimize the target function, a search for the optimal values of $D_{||}$ and $D_\perp$ was performed using the simplex algorithm (*32*); for each set of $D_{||}$, $D_\perp$, the optimal values of the Euler angles were obtained by a 1°-step grid search in the $\{\Phi, \Theta\}$ space. Confidence limits for the derived parameters were estimated using the method of constant chi-square boundaries (*32*).

Only those residues belonging to the well-defined secondary structure (*17*, *21*) were used for the analysis. Of the core residues in the SH2 domain, 61, 59, and 59 residues were effectively resolved in the free SH2, in the unligated SH(32), and in the ligated SH(32), respectively. The corresponding numbers for SH3 are 30, 29, and 30. The following residues were excluded from the analysis as either being influenced by conformational exchange or participating in slow motion as indicated by their R_2'/R_1' values beyond two standard deviations from the mean. These were S134, R135, Q160, N193, T204, and A217 in the free SH2, Q160, R161, and S148 in the unligated SH(32), and R161 and T178 in the ligated SH(32). Excluded from the analysis for the SH3 domain were I82 in the free SH3, L80 and R89 in the unligated SH(32), and K87, R89, and W99 in the ligated SH(32).

Protein Coordinates. The following protein atom coordinate sets were used for the analysis: 1abq.pdb (single Abl SH3 domain), 1abo.pdb (Abl SH3 complexed with ligand), 1abl.pdb (single Abl SH2 domain), and 2abl.pdb [Abl SH(32)]. Amide hydrogen atoms were added to crystal structures' coordinates, as necessary, using Insight II (MSI). All these coordinate sets yielded similar results (Supporting Information).

RESULTS AND DISCUSSION

The ratio, R_2'/R_1', of the experimentally determined ^{15}N relaxation rates for individual amides in the proteins under investigation is shown in Figure 1. For those residues with restricted local dynamics, both the overall hydrodynamic characteristics of the molecule and the local internuclear vector orientation can be directly derived from the observed values of the R_2'/R_1' ratio using eq 1. These measurements were obtained for the free and ligated SH(32) dual domain construct and for the individual domains, as controls. Variations in the individual values of R_2'/R_1' along the protein backbone principally reflect different orientations of the individual NH bonds with respect to the rotational diffusion frame. The observed patterns of R_2'/R_1' vs residue number (Figure 1A), reflecting changes in orientation of the rotational diffusion tensor, differ significantly between free and ligated states.

The apparent correlation time, τ_{app}, can be obtained from R_2'/R_1' for each amide group without any reference to protein structure (*33*): $\tau_{app} = (2\omega_N)^{-1}(6R_2'/R_1' - 7)^{1/2}$. In the case of isotropic rotational diffusion ($D_{||} = D_\perp$), τ_{app} coincides with the overall (isotropic) correlation time τ_c. The observed

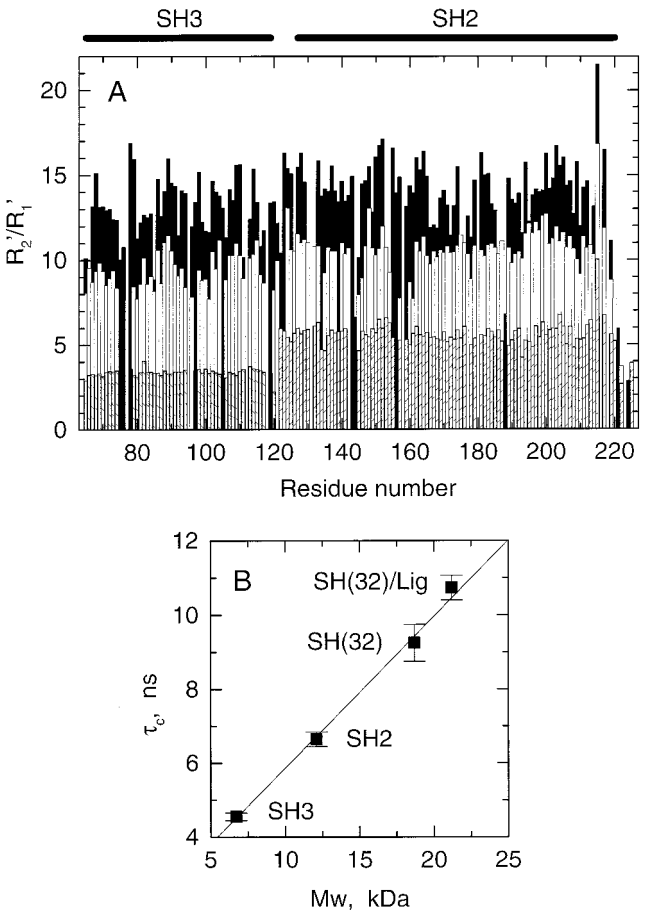

FIGURE 1: (A) Variation in the experimentally determined backbone ^{15}N R_2'/R_1' ratio versus protein sequence. Vertical bars represent the data for the unligated (white) and ligated (black) SH(32) and for the free SH3 and SH2 domains (hatching). Horizontal bars on the top indicate the location of the individual domains in the Abl SH(32) dual domain sequence. (B) Observed molecular weight dependence of the overall rotational correlation time. The two domains in SH (*32*) are not tumbling independently from each other (cf. ref *34*). Shown are the values of τ_c(ani) (Table 1), derived from the anisotropic analysis as described in the text. The values of τ_c(iso) exhibit similar dependence. The solid line corresponds to a molecular weight dependence $\tau_c = 1.76$ (±0.20) + 0.41 (±0.02) × M_w. The observed slope is comparable to 0.33, calculated from the Stokes−Einstein equation for protein density, 0.73 cm^3/g, and hydration, 0.34 g/g of H_2O.

average levels of apparent isotropic τ_{app} [column τ_c(iso), Table 1] for the free SH3, SH2, and SH(32) (9.27 ± 0.07 ns) and for the SH(32)/ligand complex (10.79 ± 0.11 ns) increase linearly with the molecular mass, 6.7, 12.1, 18.7, and 21.2 kDa, respectively, of these proteins (see also Figure 1B). Higher values of the apparent rotational correlation time for the individual domains in the dual domain construct compared to the free domains in solution suggest the presence of restricted rotational diffusion of the domains imposed by the linker. Differences in the average levels of τ_{app} in the SH3 and SH2 parts of the free dual domain construct, although small, indicate some degree of interdomain flexibility in SH(32). No significant difference was observed between the average τ_{app} values for the two domains in the SH(32)/ligand complex, consistent with restriction in the interdomain flexibility expected upon binding of the consolidated ligand. This relation between the overall tumbling times for individual domains in a dual domain protein is different from that reported in ref *34*, where large differences

Table 1: Characteristics of the Overall Rotational Diffusion of the Abl Src Homology Construct Derived from ^{15}N Relaxation Data[e]

protein	$D_\parallel/D_\perp$	Φ (deg)	Θ (deg)	E/N[a]	P[b] (%)	τ_c(ani)[c] (ns)	τ_c(iso)[d] (ns)
SH(32) unligated, subdomain SH3	1.24(0.05)	216(21)	40(10)	0.98	0.0003	8.89(0.20)	8.85(0.11)
SH(32) ligated, subdomain SH3	1.30(0.09)	212(19)	54(9)	1.26	0.59	10.51(0.51)	10.61(0.14)
SH3	1.10(0.05)	290(18)	60(12)	3.11	1.49	4.55(0.10)	4.50(0.04)
SH(32) unligated, subdomain SH2	1.16(0.04)	290(19)	38(9)	1.08	0.002	9.61(0.20)	9.49(0.07)
SH(32) ligated, subdomain SH2	1.20(0.08)	200(26)	30(13)	1.66	1.7	10.95(0.42)	10.89(0.14)
SH2	1.12(0.06)	197(17)	88(21)	1.26	3.9	6.65(0.20)	6.52(0.05)

[a] The target function E shown here was normalized by the number of degrees of freedom, which in this analysis is $N = N_r - N_{par}$, where N_r is the number of residues used and $N_{par} = 4$, representing the number of fitting parameters: τ_1, $D_\parallel/D_\perp$, Θ, and Φ. [b] P is the percentile probability that the observed improvement in fit using the anisotropic rotational diffusion model compared to the isotropic one could have occurred by chance (*48*). [c] τ_c(ani) was calculated as $\tau_c = 3\tau_1/(D_\parallel/D_\perp + 2)$, where τ_1 and $D_\parallel/D_\perp$ were derived from the orientational dependence of R_2'/R_1' for the core residues. [d] τ_c(iso) was determined as an averaged apparent individual correlation time, τ_{app}, for the core residues. [e] Numbers in parentheses indicate standard errors in the derived values. Shown in this table are results obtained using the following atom coordinates for the single protein domains: 1abo.pdb (for SH3) and 1abl.pdb (for SH2). A complete report on the results using these and other available structures is in Supporting Information.

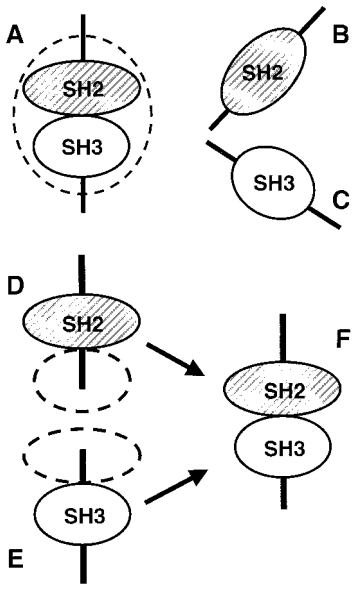

FIGURE 2: Schematic representation of the proposed method of determination of relative orientation of the domains in a dual domain protein. The overall rotational diffusion of individual domains in a multidomain protein or protein complex (A) is characterized by the common diffusion tensor; the orientation of the principal axes of this tensor may differ from those for the individual domains in a free state (B, C). The proposed method consists of, first, determination of the diffusion tensors for each of the domains in a dual domain construct separately (D, E) and, second, alignment of the rotational diffusion axes of the individual domains (F), thereby determining a proper relative orientation of the domains.

between the correlation times of the individual domains in a two-domain protein were observed, consistent with those of independent beads on a string. The rotational correlation times of the SH2 and SH3 domains in SH(32) observed here suggest the presence of certain orientational constraints between the two domains and, therefore, confirm the proposed method of characterization of interdomain orientation using relaxation data.

To quantify these observations, we determined the average orientation of the overall rotational diffusion tensor for each of the domains, using the measured R_2'/R_1' ratio. Our approach, illustrated in Figure 2, assumes that the backbone tertiary structure of the individual domains is substantially preserved in the dual domain. The amide ^{1}H and ^{15}N chemical shifts in the individual domains and in SH(32) are nearly identical (*17*). For example, only 6% of the amide groups in the SH2 and 6% in the SH3 domain exhibit a total chemical shift difference between the free state and the dual domain construct of more than 30 Hz at 600 MHz. A similar picture is observed for the ligated SH(32): only 10% of amide signals are shifted by more than 30 Hz in the SH(32)/ligand complex compared to the free SH2 bound to the ligand. Changes in orientation of amides between free and ligated SH3 in the crystal state are very small (*35*); most changes are located in the RT-Src loop. Although no structural data are currently available on the Abl SH2/ligand complex, a comparison of the crystal structures of the other SH2 domains [from Src (*36*) and from SYP tyrosine phosphatase (*37*)] in the free form and bound to various phosphotyrosine-containing peptides indicates only minor changes in the structure of the protein core. No significant changes in the result were observed when those residues in both domains involved in ligand binding were excluded from the analysis for the ligated SH(32). While clearly an approximation, the assumption that the axes can be determined from the orientations of the core of the Abl SH2 and SH3 domains is then entirely reasonable. Full structure determination, as separate domains, from the NOE data for SH(32) is in progress. The treatment used here derives a time-averaged set of anisotropic axes, and the relative orientational dependence derived is not dependent on interdomain scalar effects, such as NOE's. This analysis then fundamentally extends that of ref *4*, which assumed a time-independent, fixed relationship between subdomains.

The orientation of the principal axes of the rotational diffusion tensor with respect to the protein coordinate frame and the principal values of the tensor were determined from the measured R_2'/R_1' values, as described in Materials and Methods (see also Supporting Information). The observed rotational anisotropies for the free SH3 and SH2 domains are consistent with the ratios of the rotational diffusion tensor components, 1.14:1.02:1 and 1.17:1.04:1, respectively, calculated using the bead method (*38*, *39*). Table 1 and Figure 3 show changes in both the magnitude and orientation of the rotational diffusion tensor for each of the domains between the free state and the dual domain construct. The orientation of the diffusion axes sensed by the individual domains in the free SH(32) is consistent with the elongated conformation of the dual domain construct (Figure 3c). The relative orientation of the two domains in the SH(32)/ligand complex (Figure 3d), reconstructed from the present data, differs significantly, consistent with substantial changes in the overall spatial arrangement of the domains, induced by

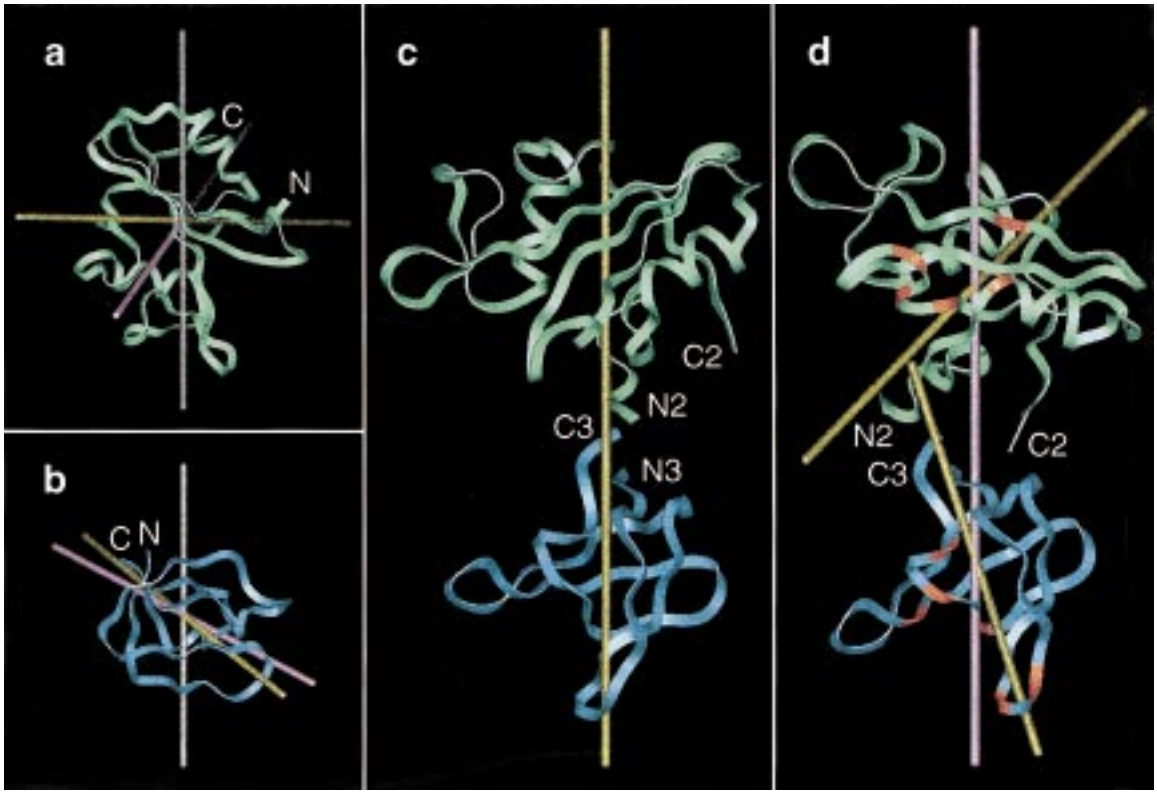

FIGURE 3: Experimental orientation of the rotational diffusion axes with respect to the domain structures. Shown are single (a) SH2 and (b) SH3 domains, and the reconstructed relative orientation of the two domains in the (c) unligated and (d) ligated Abl SH(32). The structure of the protein backbone is represented by ribbons colored green for the SH2 and blue for the SH3; the N- and C-termini are indicated. For each domain, rods represent orientations of the unique diffusion axis (corresponding to the parallel component $D_{\|}$ of the rotational diffusion tensor) in the case of the free domain (white) and in the dual domain construct, unligated (gold) and ligated (pink). The relative orientation of the individual domains in the dual domain construct was obtained by aligning the corresponding diffusion axes, as shown in parts c and d. The angle of rotation of each domain around its diffusion axis cannot be determined from these data, because of the assumed axial symmetry of the model. A rhombohedral fitting might be practical with very high precision data (*49*). In the ligated SH(32), the orientation shown was chosen to ensure proximal positioning of the ligand binding sites of the two domains (residues implicated in binding are colored red). Also shown in part d, for comparison, are orientations of the diffusion axes of the two domains as they are in the unligated SH(32). The observed change in orientation of the overall rotation axis upon ligation is 15° for the SH3 and 47° for the SH2 parts of the dual domain construct. The same optimization procedure applied to the crystal structure of Abl SH(32) (*16*), including the R_2'/R_1' data for both SH2 and SH3 domains simultaneously, resulted in the normalized target function *E/N*, which is 2.8 times greater than the corresponding values obtained here. The low probability, 6×10^{-6}, that this difference could have occurred by chance indicates differences in the relative orientations of the domains between crystal and solution studies.

the consolidated ligand. A fluorophore probe inserted in Abl SH(32) (*40*) also senses a change in conformation on ligation. Either orientation in solution is incompatible with that observed in the crystalline state (*16*). The simplest assumption is that the crystal state is different from that in solution.

The approach used here assumes that the dual domain protein can be represented by a prolate ellipsoid of revolution. The analysis used here cannot absolutely distinguish between prolate or oblate ellipsoid models (*41*). In addition, the effects of rhombicity of the rotational diffusion tensor on relaxation and averaging effects from different time scales of motion are ignored. With regard to rhombicity, its inclusion in calculations using residual dipolar couplings has been illustrated (*42*) and could be incorporated in the current analysis, by generalization to three axes of eq 1. Such analysis is in progress but is limited by the precision of data currently available for the system presented here.

With regard to time dependencies, the observed rotational anisotropy ($D_{\|}/D_{\perp}$) of the dual domain is somewhat lower than expected from rigid-body models (*43*) (e.g., compared to $D_{\|}/D_{\perp} = 1.87$ for a prolate ellipsoid of revolution with the axial ratio of 2:1); presumably the observed values are averaged by interdomain dynamics on the NMR time scale (10 ns to 100 ms). This is consistent with the different degrees of rotational anisotropy for individual domains; the $D_{\|}/D_{\perp}$ values for SH2 are somewhat smaller than for the SH3 part. Even in the SH(32)/ligand complex, where the average characteristics (τ_c, τ_{app}) of rotational diffusion for the two domains are similar, their apparent anisotropies are somewhat different, possibly due to flexibility of the ligand itself or by interconversion between bivalent and monovalent ligated forms. Similar interpretations involving interdomain mobility were reported earlier (*2*, *34*, *44*). The present results demonstrate that the relative orientation of SH2 and SH3 domains in Abl SH(32) is not fixed and can be changed by the protein interaction with a consolidated ligand. Ligand binding studies (*19*) suggest flexibility of the dual domain SH(32) construct to accommodate several relative orientations of the binding sites.

The potential range of NMR applications for deciphering the intricacies of large molecule machines in solution is considerably enhanced by the hydrodynamic characterization of proteins by ^{15}N relaxation, illustrated here for changes in domain orientations, in combination with other new methods,

especially vector orientations studied by residual dipolar coupling (*5*), relaxation-optimized spectroscopy (TROSY) (*45*), and segmental labeling (*18*, *46*, *47*).

ACKNOWLEDGMENT

We thank Drs. J. McDonnell and C. Francart and Prof. B. J. Mayer for helpful discussions. D.C. thanks members of the Cross-correlation group for discussion.

SUPPORTING INFORMATION AVAILABLE

One figure illustrating the resulting orientation dependence of R_2'/R_1', one figure with the contour maps of the optimized target function, and one table with complete statistical details of the fit. This material is available free of charge via the Internet at http://pubs.acs.org.

REFERENCES

1. Tolman, J. R., Flanagan, J. M., Kennedy, M. A., and Prestegard, J. H. (1995) *Proc. Natl. Acad. Sci. U.S.A. 92*, 9279−9283.
2. Bruschweiler, R., Liao, X., and Wright, P. E. (1995) *Science 268*, 886−889.
3. Broadhurst, R. W., Hardman, C. H., Thomas, J. O., and Laue, E. D. (1995) *Biochemistry 34*, 16608−16617.
4. Tjandra, N., Garrett, D. S., Gronenborn, A. M., Bax, A., and Clore, G. M. (1997) *Nat. Struct. Biol. 4*, 443−449.
5. Tjandra, N., and Bax, A. (1997) *Science 278*, 1111−1114.
6. Tjandra, N., Omichinski, J. G., Gronenborn, A. M., Clore, G. M., and Bax, A. (1997) *Nat. Struct. Biol. 4*, 732.
7. Clore, G. M., Starich, M. R., and Gronenborn, A. M. (1998) *J. Am. Chem. Soc 120*, 10571−10572.
8. Hansen, M. R., Rance, M., and Palmer, A. G. P. (1998) *J. Am. Chem. Soc. 120*, 11210−11211.
9. Koenig, B. W., Hu, J.-S., Ottiger, M., Bose, S., Hendler, R. W., and Bax, A. (1999) *J. Am. Chem. Soc. 121*, 1385−1386.
10. Sass, J., Cordier, F., Hoffmann, A., Rogowski, M., Cousin, A., Omichinski, J. G., Löwen, H., and Grzesiek, S. (1999) *J. Am. Chem. Soc. 121*, 2047−2055.
11. Kuriyan, J., and Cowburn, D. (1997) *Annu. Rev. Biophys. Biomol. Struct. 26*, 259−288.
12. Sicheri, F., and Kuriyan, J. (1997) *Curr. Opin. Struct. Biol. 7*, 777−785.
13. Mayer, B. J., Hirai, H., and Sakai, R. (1995) *Curr. Biol. 5*, 296−305.
14. Campbell, I. D., and Downing, A. K. (1998) *Nat. Struct. Biol. 5* (Suppl.), 496−499.
15. Deiningen, M., and Goldman, J. (1998) *Curr. Opin. Hematol. 5*, 302−308.
16. Nam, H. J., Haser, W. G., Roberts, T. M., and Frederick, C. A. (1996) *Structure 4*, 1105−1114.
17. Gosser, Y. Q., Zheng, J., Overduin, M., Mayer, B. J., and Cowburn, D. (1995) *Structure 3*, 1075−1086.
18. Xu, R., Ayers, B., Cowburn, D., and Muir, T. W. (1999) *Proc. Natl. Acad. Sci. U.S.A. 96*, 388−393.
19. Xu, Q., Zheng, J., Xu, R., Barany, G., and Cowburn, D. (1999) *Biochemistry 38*, 3491−3497.
20. Cowburn, D., Zheng, J., Xu, Q., and Barany, G. (1995) *J. Biol. Chem. 270*, 26738−26741.
21. Overduin, M., Rios, C., Mayer, B., Baltimore, D., and Cowburn, D. (1992) *Cell 70*, 697−704.
22. Xu, R., Cahill, S., and Cowburn, D. (1999) *J. Biomol. NMR* (in press).
23. Fushman, D., Cahill, S., and Cowburn, D. (1997) *J. Mol. Biol. 266*, 173−194.
24. Fushman, D., and Cowburn, D. (1998) *J. Am. Chem. Soc. 120*, 7109−7110.
25. Fushman, D., Tjandra, N., and Cowburn, D. (1998) *J. Am. Chem. Soc. 120*, 10947−10952.
26. Abragam, A. (1961) *The Principles of Nuclear Magnetism*, Clarendon Press, Oxford.
27. Farrow, N. A., Zhang, O., Szabo, A., Torchia, D. A., and Kay, L. E. (1995) *J. Biomol. NMR 6*, 153−162.
28. Woessner, D. (1962) *J. Chem. Phys. 37*, 647−654.
29. Lee, L. K., Rance, M., Chazin, W. J., and Palmer, A. G., III. (1997) *J. Biomol. NMR 9*, 287−298.
30. Copie, V., Tomita, Y., Akiyama, S. K., Aota, S., Yamada, K. M., Venable, R. M., Pastor, R. W., Krueger, S., and Torchia, D. A. (1998) *J. Mol. Biol. 277*, 663−682.
31. Fushman, D., and Cowburn, D. (1999) *J. Biomol. NMR 13*, 139−147.
32. Press, W. H., Teukolsky, S. A., Vetterling, W. T., and Flannery, B. P. (1992) *Numerical Recipes in C*, Cambridge University Press, New York.
33. Fushman, D., Weisemann, R., Thuring, H., and Ruterjans, H. (1994) *J. Biomol. NMR 4*, 61−78.
34. Hansen, A. P., Petros, A. M., Meadows, P. P., and Fesik, S. W. (1994) *Biochemistry 33*, 15418−15424.
35. Musacchio, A., Saraste, M., and Wilmanns, M. (1994) *Nat. Struct. Biol. 1*, 546−551.
36. Waksman, G., Shoelson, S. E., Pant, N., Cowburn, D., and Kuriyan, J. (1993) *Cell 72*, 779−790.
37. Lee, C.-H., Kominos, D., Jacques, S., Margolis, B., Schlessinger, J., Shoelson, S. E., and Kuriyan, J. (1994) *Structure 2*, 423−438.
38. de la Torre, J. G., and Bloomfield, V. A. (1981) *Q. Rev. Biophys. 14*, 81−139.
39. McDonnell, J. M., Fushman, D., Cahill, S. M., Zhou, W., Wolven, A., Wilson, C. B., Nelle, T. D., Resh, M. D., Wills, J., and Cowburn, D. (1998) *J. Mol. Biol. 279*, 921−928.
40. Cotton, G. J., Ayers, B., Xu, R., and Muir, T. W. (1999) *J. Am. Chem. Soc. 121*, 1100−1101.
41. Blackledge, M., Cordier, F., Dosset, P., and Marion, D. (1998) *J. Am. Chem. Soc. 120*, 4538−4539.
42. Clore, G., Gronenborn, A., and Tjandra, N. (1998) *J. Magn. Reson. 131*, 159−162.
43. Koenig, S. (1975) *Biopolymers 14*, 2421−2423.
44. Barbato, G., Ikura, M., Kay, L. E., Pastor, R. W., and Bax, A. (1992) *Biochemistry 31*, 5269−5278.
45. Pervushin, K., Riek, R., Wider, G., and Wuthrich, K. (1997) *Proc. Natl. Acad. Sci. U.S.A. 94*, 12366−12371.
46. Yamazaki, T., Otomo, T., Oda, N., Kyogoku, Y., Uegaki, K., and Ito, N. (1998) *J. Am. Chem. Soc. 120*, 5591−5592.
47. Yu, H. (1999) *Proc. Natl. Acad. Sci. U.S.A. 96*, 332−334.
48. Draper, N. R., and Smith, H. (1981) *Applied regression analysis*, John Wiley and Sons, New York.
49. Clore, G. M., Gronenborn, A. M., Szabo, A., and Tjandra, N. (1998) *J. Am. Chem. Soc. 120*, 4889−4890.

BI990897G